12WCEE 2000

0952

DYNAMIC BEHAVIOR IN LONGITUDINAL DIRECTION OF SHIELD TUNNEL LOCATED AT IRREGULAR GROUND WITH CONSIDERING EFFECT OF SECONDARY LINING

Atsushi KOIZUMI[1] And Chuan HE[2]

SUMMARY

This paper describes the seismic behavior in the longitudinal direction of shield tunnels located at an irregular ground with considering the effect of the secondary lining. A series of shaking table model tests was carried out and the response analyses of the shield tunnel were performed with emphasis on the time-history seismic deformation method. The investigation concerns vibration characteristics of the tunnel and the surrounding ground, the dynamic interaction between tunnel and ground, as well as the validity of the analytical model. In the model tests, the irregular ground with an inclined interface between alluvium and diluvium was considered, and the longitudinal rigidity of the tunnel with the secondary lining and the exciting direction were focused, moreover materials of ground and tunnel were chosen according to the similarity law. In the response analyses, the time-history response displacements of the free ground were analyzed by using 3-D dynamic FEM and the 1-D multiple reflection response method, respectively. An analytical model in the longitudinal direction of the shield tunnel with the secondary lining for the seismic deformation method was proposed and the validity of the model is verified by model tests.

INTRODUCTION

Shield tunnels are utilized widely in urban areas as the lifeline in Japan. However, these areas are almost located at high earthquake intensity regions and encountered frequent seismic attack in the past. Recent years, attention has been paid by engineers to carry out the seismic design of shield tunnels. Currently, the seismic deformation method for seismic design of shield tunnels in the longitudinal direction has been suggested, and the response displacement of ground is assumed as a simple sinusoidal distribution [2], obviously it is not suitable for irregular ground. In the meantime, in order to correct the longitudinal meander of the segment, and achieve waterproof and rustproof effect, the secondary lining is employed widely. Investigations about vibration characteristics of the tunnel and the surrounding ground, the dynamic interaction between tunnel and ground, as well as a proper analytical model with considering the effect of the secondary lining are insufficient now [1]. In order to make a thorough study on these aspects, in this paper, a series of shaking table model tests was carried out and the response analyses of the shield tunnel were performed.

SHAKING TABLE MODEL TESTS

Prototype of tunnel and ground:

A single-track subway shield tunnel with the secondary lining was selected as the prototype, which is located at an irregular ground with an inclined interface between alluvium and diluvium. The outer diameter of the shield tunnel is 7.0m, the inside diameter is 5.8m. The segment is a RC flat plate type, whose width and thickness is 1m and 0.4m, respectively. The secondary lining is the cast-in-place plain concrete, whose thickness is 0.2m.

[1] *Department of Civil Engineering, Waseda University, Tokyo Japan Email: koizumi@mn.waseda.ac.jp*
[2] *Department of Civil Engineering, Waseda University, Tokyo 169-8555, Japan Facsimile: +81-3-3204 1946*

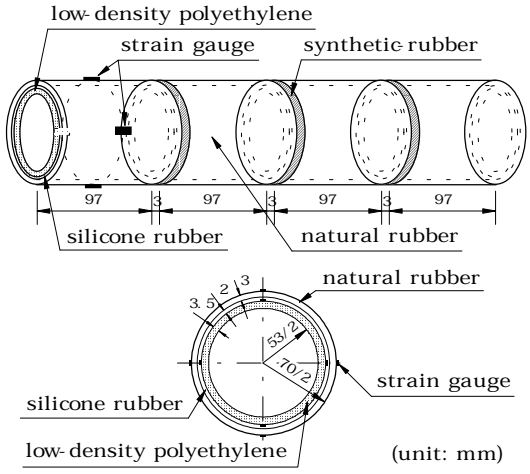

Figure 1: Details of tunnel model.

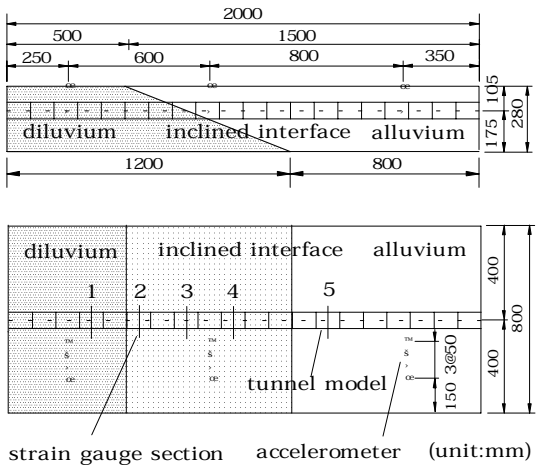

Figure 2: Details of ground model.

Similarity Law:

In the model tests, materials of ground and tunnel were chosen according to the similarity law. The similarity law of the physical quantity is introduced as follows. First, It is assumed that the inertial force and the elastic force in the ground is the mutually independent dominant physical quantity. They can be shown in equation (1) and equation (2) using mass density length ƒÏ, time t, ł, strain and ƒÎ elastic modulus E.

$$F_i = f\ddot{I} \cdot l^4 \cdot t^{-2} \tag{1}$$

$$F_s = f\tilde{A}E \cdot l^2 \tag{2}$$

The similar relation between prototype and model is shown as Equation (3) using the ratio of these forces:

$$\frac{f\ddot{I}_m \cdot l_m^2}{f\tilde{A}_m \cdot E_m \cdot t_m^2} = \frac{f\ddot{I}_p \cdot l_p^2}{f\tilde{A}_p \cdot E_p \cdot t_p^2} \tag{3}$$

Where subscript m and p denotes model and prototype respectively.
Next, the similarity law of mass density, length and elastic modulus is considered as the basic similarity law respectively, which is shown in Equation (4).

$$P = \frac{f\ddot{I}_m}{f\ddot{I}_p}, \quad L = \frac{l_m}{l_p}, \quad e = \frac{E_m}{E_p} \tag{4}$$

Finally, we fix that dimensionless quantity (strain) is equivalence, then the similarity law of time (t_m/t_p) and similarity law of acceleration (a_m/a_p) can be introduced as following Equation (5).

$$\frac{t_m}{t_p} = L \cdot \sqrt{\frac{P}{e}}, \quad \frac{a_m}{a_p} = \frac{e}{P \cdot L} \tag{5}$$

The similarity law and similar ratio of the physical quantity are shown in Table 1.

Model of tunnel and ground:

In order to facilitate the manufacturing of the tunnel model with many transverse and circumferential joints, each 10 number of segment rings was reduced to one segment ring with an equivalent rigidity considering the effect of transverse and circumferential joints [3,4]. Natural rubber rings and synthetic rubber rings was used respectively as the equivalent tunnel segment ring and the equivalent ring joint. A low-density polyethylene tube was used as the secondary lining. Moreover, in order to simulate the transmission effect of the waterproof sheet between segment and secondary lining, the interval between segment and secondary lining was filled by silicone rubber. Details of the shield tunnel model are shown in Figure 1. The plan size of the ground model was 2000× 800mm, the height was 280 mm. Alluvium and diluvium was simulated respectively with using two types of silicone rubbers. Details of the ground model are shown in Figure 2. The elastic moduli of the model materials are shown in Table 2.

Test case and excitation:

TABLE 1: SIMILARITY LAW.

	Basic similarity law			Introduced similarity law		
	Density	**Length**	**Elastic modulus**	**Time**	**Acceleration**	**Strain**
Law	$P = \rho_m / \rho_p$	$L = l_m / l_p$	$e = E_m / E_p$	$L \cdot (P/e)^{1/2}$	$e/(P \cdot L)$	$\varepsilon_m / \varepsilon_p$
Ratio	1.0/1.8	0.01	0.01	7.5×10^{-2}	1.8	1.0

Table 2: Elastic modulus (unit: N/mm^2).

	Alluvium	**Diluvium**	**Segment**	**Joint**	**Secondary lining**
Prototype	10	75	297.6	81.02	2.7×10^4
Based on law	0.1	0.75	2.976	0.8102	2.7×10^2
Model	0.12	0.73	2.8	0.98	3.5×10^2

Table 3: Test case.

Exciting direction	**Free ground model without tunnel**	**Tunnel-soil composite model without secondary lining**	**Tunnel-soil composite model with secondary lining**
Transverse	Test D	Test D1	Test D2
Longitudinal	Test F	Test F1	Test F2

Shaking table tests were carried out for both the free ground model and the tunnel-soil composite model with and without the secondary lining, respectively. The bottom of the model was fixed to the shaking table, and the unidirectional horizontal exciting wave was inputted from the shaking table in the transverse direction and the longitudinal direction, respectively. First, the model was excited by the sinusoidal wave, in which, the maximum acceleration was 50gal, and the frequency was changed from 2Hz to 20Hz. Second, Tokachi-Oki earthquake record (Hachinohe) was used as the exciting seismic wave, whose time base was shortened to 1/5 in real time, maximum amplitude was normalized to 100gal. Table 3 lists test cases.

Measurement item:

Accelerometers, which record the absolute time-history accelerations in the transverse and longitudinal direction, were put on the ground surface and the underground (see Figure 2). Strain gauges, which record the longitudinal time-history strains of the tunnel, were put on 5 cross sections of the tunnel model (see Figure 1 and Figure 2). The maximum displacements of the ground surface and the underground in the transverse and longitudinal direction were measured by blurring photographs (sinusoidal excitation only).

METHOD OF NUMERICAL ANALYSIS

The numerical simulations were carried out on the shaking table tests. The time-history seismic deformation method in a wide sense was employed in the response analyses of the shield tunnel. Time-history response displacements of the free ground, which were calculated based on the 3-D FEM dynamic analysis or the 1-D earthquake response of horizontally layered sites, were inputted statically to the analytical model of the tunnel through the ground springs.

Analytical model of tunnel:

The static model in the longitudinal direction of the shield tunnel with considering the effect of the secondary lining is shown in Figure 3. The segment and the secondary lining were simulated by the beam-spring structural model in which the beam elements and spring elements were positioned alternately. The beam element for the

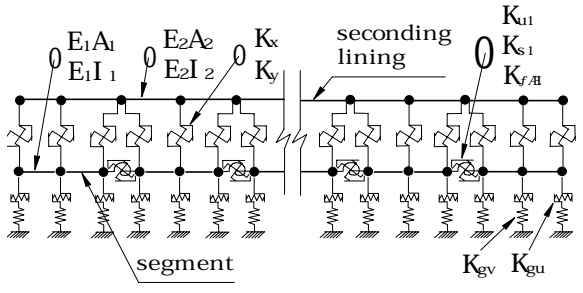

Figure 3: Analysis model of tunnel.

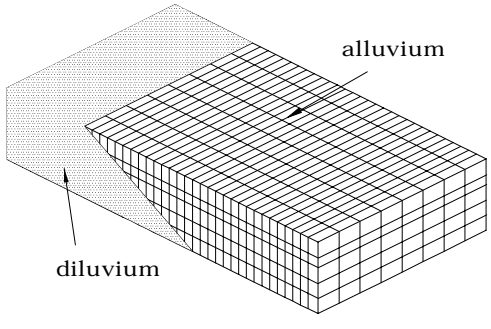

Figure 4: dynamic FEM model of ground.

segment was estimated by the equivalent longitudinal tension-compression rigidity and the equivalent bending rigidity; the beam element for the secondary lining was estimated by the longitudinal tension-compression rigidity and the bending rigidity. In the meantime, the circumferential joint of the segment ring was simulated by the tension-compression spring element, the shear spring element and the rotation spring element, moreover, the interaction between segment and secondary lining was simulated by the shear spring element and the compression spring element, the interaction between tunnel and ground was simulated by the shear spring element and the compression spring element.

Spring constants for circumferential joints:

According to the relationship between deformation and force of a synthetic rubber ring (which simulated the circumferential joints of a segment ring in the tests), spring constants (tension-compression K_{u1}, shear K_{s1}, rotation $K_{f\AE}$) of the circumferential joint of a segment ring can be determined by Equation (6),

$$K_{u1} = \frac{E_g A_g}{l_g}, \quad K_{s1} = \frac{E_g A_g}{2(1+f\ddot{E}_g)\cdot l_g}, \quad K_{f\AE} = \frac{E_g I_g}{l_g} \tag{6}$$

where, E_g, A_g, l_g, I_g and $f\ddot{E}_g$ denotes elastic modulus, sectional area, width, geometrical moment of inertia and Poisson's ratio of the synthetic rubber ring, respectively.

Spring constants estimating interaction between segment and secondary lining:

The shear interaction between segment and secondary lining is simulated by the shear spring element, and spring constant K_x of the shear spring can be determined by Equation (7),

$$K_x = \frac{K_{x1}\cdot K_{x2}}{K_{x1}+K_{x2}+\dfrac{K_{x2}\cdot K_{x1}}{K_{xiso}}} \tag{7}$$

where, K_{x1}, K_{x2}, K_{xiso} can be determined by following equations,

$$K_{x1} = \frac{E_1\cdot A_x}{2(1+f\ddot{E}_1)t_1}, \quad K_{x2} = \frac{E_2\cdot A_x}{2(1+f\ddot{E}_2)t_2}, \quad K_{xiso} = \frac{E_{iso}\cdot A_x}{2(1+f\ddot{E}_{iso})t_{iso}} \tag{8}$$

where, E_1, E_2, E_{iso} denotes the elastic modulus of segment, secondary lining, as well as waterproof sheet (this sheet was simulated by silicone rubber in the tests), respectively. t_1, t_2, t_{iso} denotes the thickness, $f\ddot{E}_1$, $f\ddot{E}_2$, $f\ddot{E}_{iso}$ denotes the Poisson's ratio, respectively. A_x denotes the outer periphery area of the secondary lining between nodes of a beam element (see Figure 3).

The compression interaction between segment and secondary lining is simulated by the compression spring element, and spring constant K_y of the compression spring can be determined by Equation (9) [5],

$$K_y = \frac{K_{y1}\cdot K_{y2}}{K_{y1}+K_{y2}+\dfrac{K_{y2}\cdot K_{y1}}{K_{yiso}}} \tag{9}$$

where, K_{y1}, K_{y2}, K_{yiso} can be determined by following equations,

$$K_{y1} = \frac{2E_1\cdot A_y}{t_1}, \quad K_{y2} = \frac{2E_2\cdot A_y}{t_2}, \quad K_{yiso} = \frac{E_{iso}'\cdot A_y}{t_{iso}} \tag{10}$$

where, E_{iso}' denotes the restricted elastic modulus of the waterproof sheet, and E_{iso}' should be measured by using the uniaxial compression test by restricting the circumferential deformation of the specimen. A_y denotes the outer level projecting area of the secondary lining between nodes of a beam element (see Figure 3).

Ground spring constants:

Because the sliding displacement between the tunnel and the ground has been restricted in the tests, it can be assumed that ground springs are linear springs. Hence, the plate-loading test is concluded to determine ground spring constants. The compression ground spring constant (K_{gv}) and the shear ground spring constant (K_{gu}) can be determined by Equation (11) and Equation (12), respectively.

$$K_{gv} = \frac{1}{2} k_g \cdot D_1 \cdot B \tag{11}$$

$$K_{gu} = \frac{1}{2} \cdot \frac{1}{2(1+\nu)} k_g \cdot \nu \cdot D_1 \cdot B \tag{12}$$

where, k_g denotes the coefficient of subgrade reaction of the model ground, and D_1 , ν, B, denotes outer diameter of model tunnel, node interval of beam element shown in Figure 3, Poisson's ratio of the model ground.

Dynamic response analysis of free ground:

In the 3-D FEM dynamic analysis, the step by step integration method was used with β=1/4 of the Newmark's β scheme, and the wave damping of Reyleigh type was employed. Input excitations were time-history

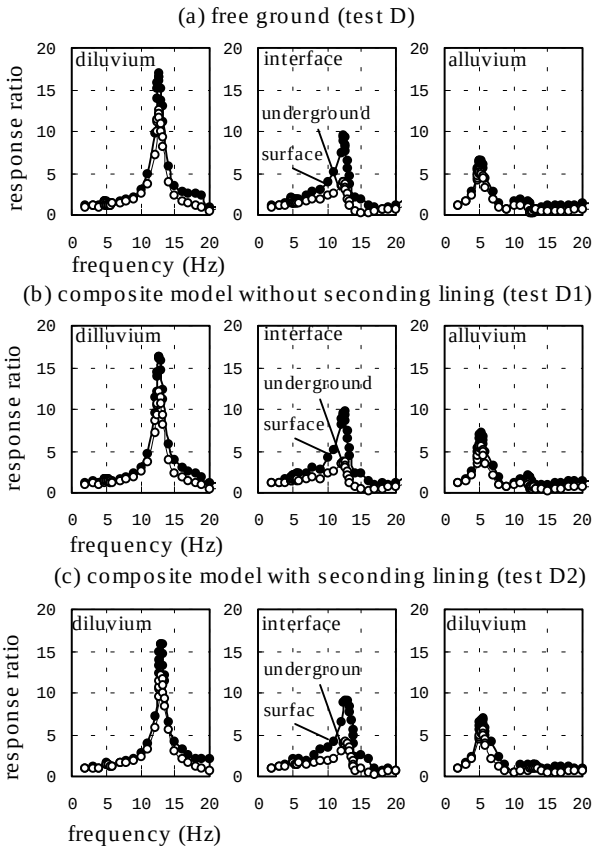

Figure 5: Resonance Curves Of Ground Accelerations

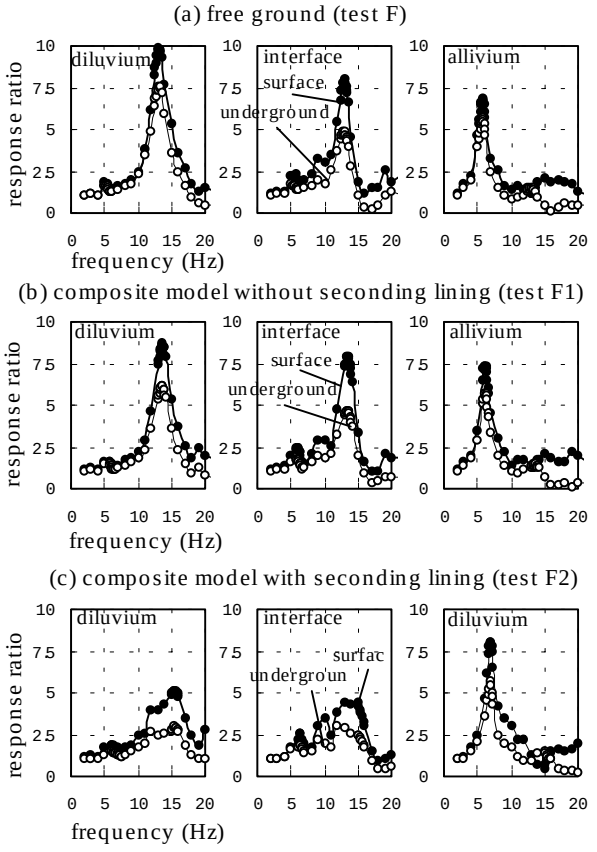

Figure 6: Resonance Curves Of Ground Accelerations

accelerations of the shaking table, which had been measured from the shaking table test. Figure 4 shows the finite element idealization of the ground model for the 3-D dynamic analysis.

It is considered that the maximum ground displacement differences should come out in the vicinity of the inclined interface. Then the inclined interface ground is divided into many small grounds, and it is assumed that these grounds divided are mutually independent. The 1-D dynamic response analysis of horizontally layered sites based on the multiple reflection theory was used to calculate response displacements of the free ground.

TEST RESULTS FOR SINUSOIDAL EXCITATION

Resonance curves of ground accelerations:

The resonance curves of ground accelerations are shown in Figure 5 and Figure 6. It can be seen that, if the model is excited in the transverse direction (see Figure 5), for each test case (test D, test D1 and test D2), the shape of resonance curve of the ground acceleration, the maximum response ratio of the acceleration, as well as the resonant frequency are almost same at each corresponding place. However, if the model is excited in the longitudinal direction (see Figure 6), for test F and test F1, the shape of resonance curve of the ground acceleration, the maximum response ratio of the acceleration and the resonant frequency do not almost change at each corresponding place (test F and test F1), but for test F2, all of these change greatly. The results indicate

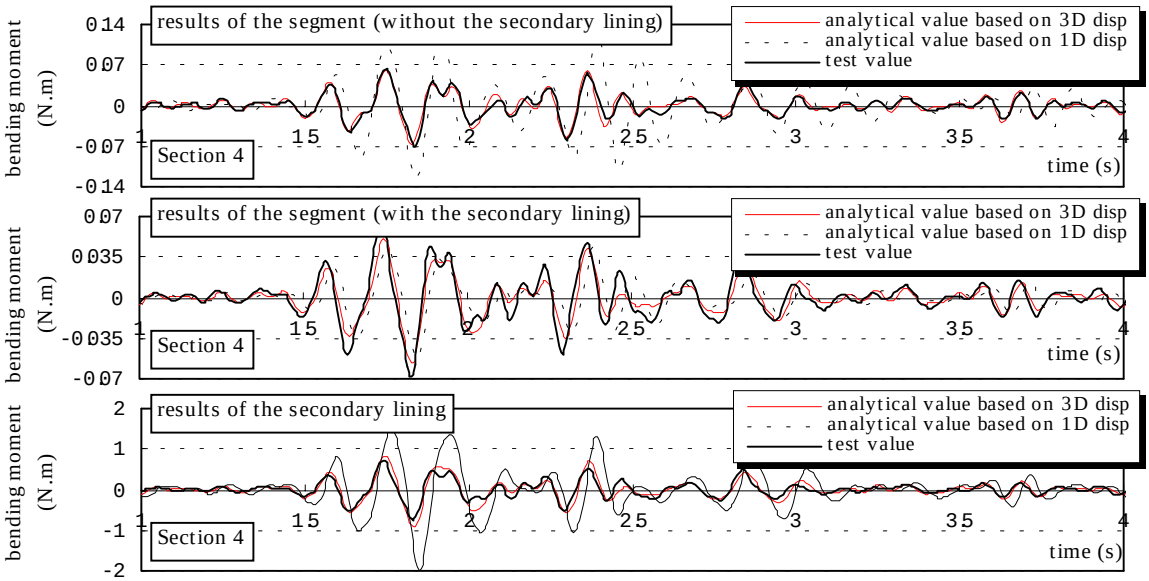

Figure 9: Test and analytical results of the longitudinal bending moment of the tunnel.

that, when a shield tunnel without the secondary lining is constructed, the dynamic behavior of the surrounding ground does not almost change whether the ground is excited in the transverse direction or in the longitudinal direction. In the meantime, when a shield tunnel with the secondary lining is constructed, the dynamic behavior of the surrounding ground does not almost change if the ground is excited in the transverse direction, but change greatly if the ground is excited in the longitudinal direction.

Distribution of ground displacements:

The maximum displacement distribution of the ground (result for center depth of tunnel) under the transverse excitation with resonant frequency of alluvium is shown in Figure 7, and that under the longitudinal excitation is shown in Figure 8. From Figure 7 it can be observed that, the maximum displacement distribution of each transverse position of the ground for each test case is almost same. From Figure 8 it can be observed that, in test F each transverse position of the ground has almost a equally maximum displacement, and in test F1 the maximum displacement in the vicinity of the tunnel is slightly less than other position of the ground, but in test F2 the maximum displacement in the vicinity of the tunnel is much less than other position of the ground, moreover, in both test F1 and test F2 the displacement distribution in the side of the ground is almost same.

Table 4: Dominant frequency of tunnel strain response and resonant frequency of ground (unit: Hz).

Resonant frequency of ground			Strain dominant frequency			Strain dominant frequency		
Test D	diluvium	12.6	**Test D1**	Section 1	14.65	**Test D2**	Section 1	14.65
	interface	12.5		Section 4	4.49		Section 4	6.35
	alluvium	5.2		Section 5	6.30		Section 5	6.35
Test F	diluvium	12.9	**Test F1**	Section 1	14.5	**Test F2**	Section 1	6.35
	interface	12.9		Section 4	6.30		Section 4	6.35
	alluvium	5.7		Section 5	6.30		Section 5	6.35

We can confirm that, first, under the transverse excitation the tunnel follows the free ground in the displacement distribution whether with or without a secondary lining. Second, under the longitudinal excitation, generally the tunnel without a secondary lining follows the free ground in the displacement distribution, but the tunnel with a secondary lining does not follow the free ground in the displacement distribution, in other words, in this case the surrounding ground is restricted by the tunnel.

TEST AND ANALYTICAL RESULTS FOR SEISMIC EXCITATION

Test results of strain response characteristics of tunnels:

The dominant frequency of the tunnel strain response (values of Section 1, 4, 5, calculated from Fourier spectrum) and resonant frequency of the ground (calculated from Figure 5 and Figure 6) are shown in Table 4. From this table, one can observe that in both test D1 and test F1, the dominant frequency of strain response of Section 1 is close to the resonant frequency of diluvium and Section 4, 5 close to alluvium, results of test D2 are similar to test D1 or test F1, but in test F2 all Sections close to alluvium.

From this result it is shown that, if the secondary lining is not added, in both alluvium and diluvium the tunnel follows respectively the corresponding surrounding ground in the dynamic behavior, and in the vicinity of the inclined interface the tunnel follows alluvium, which are irrelevant to the exciting direction. If the secondary lining is added, under the transverse excitation the dynamic behavior of the tunnel does not change any, however, under the longitudinal excitation the entire tunnel follows alluvium in the dynamic behavior.

Test and analytical results of sectional forces of tunnels:

Test result and analytical result of the longitudinal bending moment of the segment and the secondary lining of the tunnel are shown in Figure 9, and the longitudinal axial force are shown in Figure 10 (only take result of Section 4 in 1-4 second for example). From these figures, One can observe that the analytical value based on the

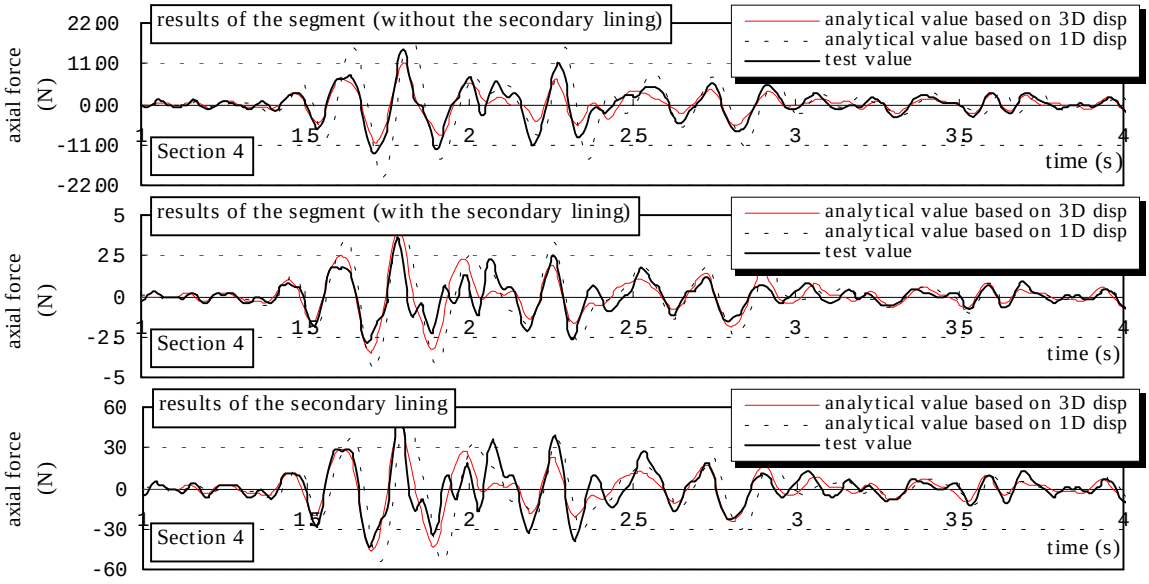

Figure 10: Test and analytical results of the longitudinal axial force of the tunnel.

displacements of the 3-D FEM dynamic analysis is found to be in good agreement with the test value both the axial force and the bending moment, however, the analytical value based on the displacements of the 1-D dynamic response analysis of horizontally layered sites does not coincide the test value.

In the meantime, when a secondary lining is added, the longitudinal axial force of the segment decreases drastically, but the longitudinal bending moment of the segment does not change. It means that the segment can be reinforced by a secondary lining under longitudinal excitation but cannot under transverse excitation.

CONCLUSIONS

1. In the irregular ground, the transverse dynamic behavior of surrounding ground does not almost change even if a shield tunnel with the secondary lining is constructed; the shield tunnel follows the corresponding surrounding ground in the transverse dynamic behavior. But the longitudinal dynamic behavior of the surrounding ground is influenced significantly by the shield tunnel with the secondary lining; in general, if the resonant frequency of a ground is close to the dominant frequency of the seismic motion, the shield tunnel will follow this ground in longitudinal dynamic behavior.

2. Under the transverse excitation, displacements of shield tunnels are almost irrelevant to the rigidity of the secondary lining, which are close to that of the free ground, but under the longitudinal excitation displacements of shield tunnels are significantly related to the rigidity of the secondary lining, displacements of shield tunnels with a secondary lining are much less than that of the free ground. This phenomenon should be considered as a key point in the seismic design of a shield tunnel with the secondary lining.

3. When accurate response displacements of free ground are employed, the calculating longitudinal sectional forces based on the analytical model of a shield tunnel with a secondary lining proposed by authors agree with the test values, the validity of the analytical model is verified.
4. In the irregular ground, to ensure the calculating accuracy of sectional forces of shield tunnels in the longitudinal direction, accurate response displacements of the free ground are required. Response displacements based on the 3-D FEM dynamic analysis have good accuracy, but based on the multiple reflection response analysis can not satisfy necessary accuracy.
5. When the secondary lining is added, the longitudinal axial force of the segment decreases drastically, but the longitudinal bending moment of the segment does not change; the secondary lining has a reinforcing effect for the segment under longitudinal excitation, but has nothing under transverse excitation.

REFERENCES

1. He, C and Koizumi, A. (1999), “Seismic behavior in longitudinal direction of shield tunnel located at irregular ground”, *Proceedings of the 1st International Conference on Advances in Structure Engineering and Mechanics*, Seoul.
2. JSCE (1996), *The Tunnel Standard Specifications (The Shield Tunneling Edition)*, pp49-53. (in Japanese)
3. Murakami, H. and Koizumi, A. (1980), “On the behavior of transverse joints of a segment”, *Proceedings of JSCE*, No.296, pp73-86. (in Japanese)
4. Nishino, K., Koizumi, A. and Murakami, H. (1989), “Study on shield tunnel lining design by taking into account of segment joint characteristics”, *Proceedings of International Congress on Progress and Innovation in Tunnelling*, Toronto, pp277-285.

Takamatsu, N., Murakami, H. and Koizumi, A. (1992), “A study on the bending behavior in the longitudinal direction of shield tunnels with secondary linings”, *Proceedings of ITA Congress Towards New Worlds in Tunnelling*, Acapulco, pp537-544.